Korean J. Chem. Eng., 35(2), 375-382 (2018)
DOI: 10.1007/s11814-017-0305-9

pISSN: 0256-1115
eISSN: 1975-7220

Transformation of nitrogen-containing compounds in atmospheric residue by hydrotreating

Mei Liu*,†, Lin-Zhou Zhang, Cheng Zhang***, Sheng-Hua Yuan***, De-Zhi Zhao*, and Lin-Hai Duan***

*College of Chemistry, Chemical Engineering and Environmental Engineering, Liaoning Shihua University, Fushun 113001, China
**State Key Laboratory of Heavy Oil Processing, China University of Petroleum, Beijing 102249, China
***Fushun Research Institute of Petroleum and Petrochemicals, SINOPEC, Fushun 113001, China
(*Received 20 April 2017 • accepted 5 November 2017*)

Abstract−Atmospheric residue from Saudi Arabia light crude oil was subjected to the hydrotreating process in a continuous fixed-bed reactor with hydrodesulfurization (HDS) and hydrodenitrogenation (HDN) catalysts. The detailed molecular composition of the polar heteroatom species in the feedstock and products was determined by electrospray ionization (ESI) Fourier transform ion cyclotron resonance mass spectrometry (FT-ICR MS) combined with other analytical methods. The ESI FT-ICR MS analysis indicates that the N_1 class species have the highest relative abundance. In the hydrotreating process, small neutral N_1 class species with high aromaticity and short side chains showed the highest relative abundance and were defined as easily removable compounds. High aromaticity and small molecule basic N_1 compounds exhibited higher catalytic activity towards hydrogenation. The N_1S_1 class species were converted to the N_1 class species, or even hydrocarbons, by the preferential removal of the sulfur atoms. Most of the N_1O_1 class species were difficult to remove, because of their stable chemical structure.

Keywords: Atmospheric Residue, Hydrodesulfurization (HDS), Hydrodenitrogenation (HDN), Fourier Transform Ion Cyclotron Resonance Mass Spectrometry (FT-ICR MS)

INTRODUCTION

Petroleum is a non-renewable and valuable energy resource [1]. The key to improving the utilization of petroleum resource is the complete transformation of its residue [2]. Residue hydrogenation process is considered as the most effective method to remove the sulfur residue owing to its flexible process solutions and strong applicability of the raw material [3,4]. The fixed-bed residue hydrotreating technology is well developed, easy to operate, and has the capacity of handling most of the residual feedstocks [5]; therefore, the development of efficient fixed-bed residue hydrogenation technology is still important for the production of light fuel and environmental protection in the future [6,7].

For more accurate understanding of residue hydrogenation technology and achieving complete and high efficiency transformation, the study of microscopic to macroscopic characteristics of residue is necessary. The common analysis methods of residue include infrared spectroscopy [8-10], wave spectrum [11,12], fluorescence spectroscopy [13], and mass spectrometry [14-17]. These analytical tools provide information about compositions, average molecular structure, narrow fraction properties, and side chain structure of saturates, aromatics, resins, and asphaltenes (SARAs), and have been extensively used to delineate the structure of hydrocarbons and non-hydrocarbon components in the residue from various aspects for a preliminary understanding of the structure and composition of these molecules. However, these methods can only infer some of the details of the molecular structure of heavy oil. The structural information at the molecular level and the essential attribute has not been revealed.

High-resolution Fourier transform ion cyclotron resonance mass spectrometry (FT-ICR MS) has made possible to understand heavy oil at the molecular level [18-23]. This mass spectrometric technique has been used to understand the molecular transformation of heavy oil hydrogenation [24-28]. Based on previous investigations, a continuous mini-fixed-bed reactor was used in this study. The process conditions fully simulate the operating conditions of industrial plants, using diverse industrial catalysts. Indepth study of the residue hydrotreating process and the common and characteristic transformation laws of polar compounds (especially N-containing compounds) during the hydrotreatment of residue are summarized at the molecular level.

EXPERIMENTAL

1. Feedstock

Atmospheric residue from Saudi Arabia light oil (SQAR, 350 C^+ fraction) was used as the feedstock, and the description and bulk property of the feedstock are listed in Table 1.

2. Hydrotreating Experiments

The feedstock was subjected to a hydrotreating test in a 30-mL mini fixed-bed reactor packed with two commercial catalysts. The hydrotreating process of the feedstock is shown in Fig. 1. The process comprises two sections, the hydrodesulfurization (HDS) and hydrodenitrogenation (HDN) catalysts connected in series. Two

†To whom correspondence should be addressed.
E-mail: liumeifushun@163.com

Table 1. Bulk properties of feedstock and hydrotreating products

Properties	Feedstock	HDS-product	HDN-product
Density (20 °C)[a], g/cm^3	0.9790	0.9492	0.9450
Conradson carbon residue (CCR)[b], m%	12.23	7.80	6.85
Viscosity (100 °C)[c], mPa·s	78.41	36.9	35.26
Molecular weight[d]	586	380	566
Carbon[e], wt%	85.06	86.31	86.48
Hydrogen[e], wt%	10.95	11.57	11.63
Nitrogen[f], wt%	0.30	0.24	0.20
Sulfur[g], wt%	3.15	1.10	1.01
Nickel[h], μg/g	17.95	8.197	6.671
Vanadium[h], μg/g	54.49	13.92	11.42

[a]GB/T 13377-1992
[b]SH/T0170-92
[c]GB/T 11137
[d]SHT0398 (VPO)
[e]SH/T0656-98 (04)
[f]SH/T0704-2001
[g]SH/T0689-2000
[h]ASTM D5708

commercial NiMo/Al_2O_3 catalysts were used. The composition of the catalysts has been described elsewhere [29]. The catalysts were presulfided with 2% carbon disulfide in cyclohexane for 72 h, followed by precoking with aviation kerosene for 48 h. According to the performance of the catalysts and requirements of the products, experiments were conducted under the following initial conditions for this atmospheric residue (AR): temperature, 360 °C; hydrogen pressure, 14.7 MPa; liquid hourly space velocity (LHSV), 0.25 h^{-1}; and H_2/feed ratio, 650 : 1 (m^3/m^3). Analysis data reported for each data point were obtained after at least 24 h time-on-stream under a given set of conditions. Fresh catalysts were used for each feed. Depending on the number of data points collected, sometimes two fresh catalysts were used for the same heavy oil feed, to avoid any significant contribution from deactivation. For convenience, the liquid products from the outlets of reactors 1 and 2 were named as HDS-product and HDN-product, respectively.

3. ESI FT-ICR MS Analysis

Samples were dissolved in a mixture of toluene and methanol (4 : 6, v/v) at a concentration of 0.2 mg/mL. To enhance the ionization efficiency, 15 μL NH_4OH (Analytical reagent, 28-33 wt%) and 10 μL formic acid (AR, 98 wt%) were added. MS analysis was performed using a Bruker Apex-ultra FT-ICR mass spectrometer equipped with a 9.4 T superconducting magnet. Using a syringe pump, the samples were injected into the ESI source at 180 μL/h. The atomizing and drying gas flow rates were 1.2 and 5 L/min, respectively. The operating conditions for positive-ion (or negative-ion) formation were −3.5 kV (or 4 kV) polarization voltage. The emitter and capillary column end voltages were −4.0 kV (or 4.5 kV) and 320 V (or −320 V), respectively. The optimized mass for Q1 was 250 Da and 300 Vp-p RF amplitude. The key operating parameters were in 100-1,000 mass range, and the acquired data size was 4 M, in which ions accumulated for 0.1 s (or 0.2 s). The time domain data sets were co-added from 128 data acquisitions.

Over 20,000 different polar organic compounds with different elemental composition ($C_cH_nN_nO_oS_s$) were observed. The compound "class" is directly defined as the number of heteroatoms in the molecule. For example, N_1 class species refers to the compounds with one nitrogen atom.

The mass calibration and data analysis have been described elsewhere [26]. Briefly, the mass spectra were internally calibrated by N_1 class homologous using commercial software. Mass spectra peaks with relative abundance six times less than the standard deviation of baseline noise were removed in the calculation for simplification.

RESULTS AND DISCUSSION

1. Bulk Property

Table 1 shows the bulk properties of SQAR and its hydrotreat-

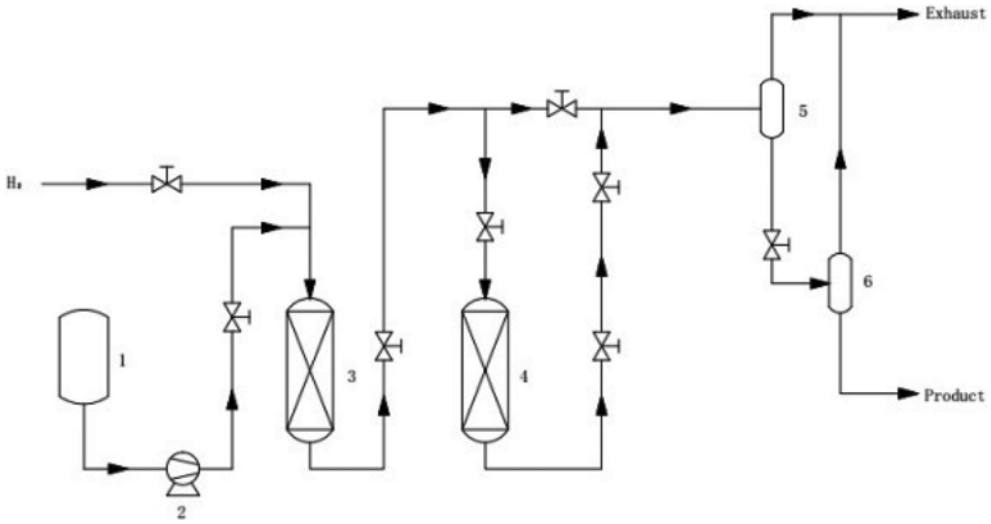

Fig. 1. Flow chart of residue hydrotreating.
1. Feed tank 2. Feed pump 3. Reactor 1 4. Reactor 2 5. Buffer tank 6. High pressure separtor

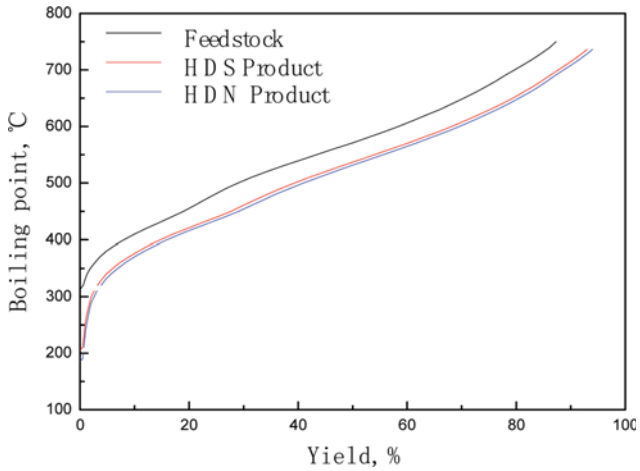

Fig. 2. Simulated distillation curves of feedstock and hydrotreating products.

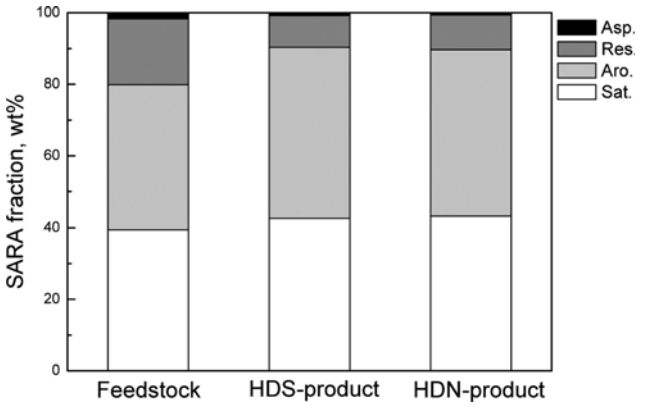

Fig. 3. SARA of feedstock and hydrotreating products.

ing products. After the hydrotreating process, the nitrogen (N), sulfur, vanadium, and nickel content showed a steady decrease with increasing hydrotreating depth. Fig. 2 shows the simulated distillation curve of feedstock and different outlet hydrotreating liquid products. As shown, the boiling range distribution of feedstock and products changed only slightly during the entire hydrogenation process. The aim of the process was to remove the impurities to ensure a few cracking and condensation reactions. Only a small amount of light oil was obtained, and coke yields were lower than those of the hydrocracking reactions.

Fig. 3 shows the SARA compositions of the feedstock and HDS and HDN products. With increasing hydrogenation depth, the saturated and aromatic contents increased, whereas those of resin and asphalt decreased. The conversion of the SARAs did not complete. First, many resins and asphaltenes were converted to aromatics, saturated compounds, or cokes. The aromatics and saturates increased significantly. With the progress of the reaction, the aromatics further transformed to saturated components. Thus, the aromatics in the samples decreased, and saturated components continued to increase. From the SARA analysis, it is expected that the polarity of the products decreased as with intense hydrotreating process.

2. Molecular Composition Characterized by Negative-ion ESI FT-ICR MS

Polar heteroatom compounds in the feedstock as well as in the hydrotreating products from different reactor outlets were analyzed by ESI FT ICR-MS under the negative ion mode. The broadband and the expanded scale mass spectra segments at m/z 354 are shown in Fig. 4, indicating that the mass spectra for the feedstock exhibit a distinct bimodal distribution with the centers of the spectrum peaks at m/z 340 and 400, corresponding to the N_1 and O_2 class species, respectively. With increasing depth of the hydrotreatment reactor, the peaks of the O_2 class species (carboxylic acids) disappeared and those of N_1 species class shifted to higher mass ranges. The carboxylic acid derivatives were easily removed during

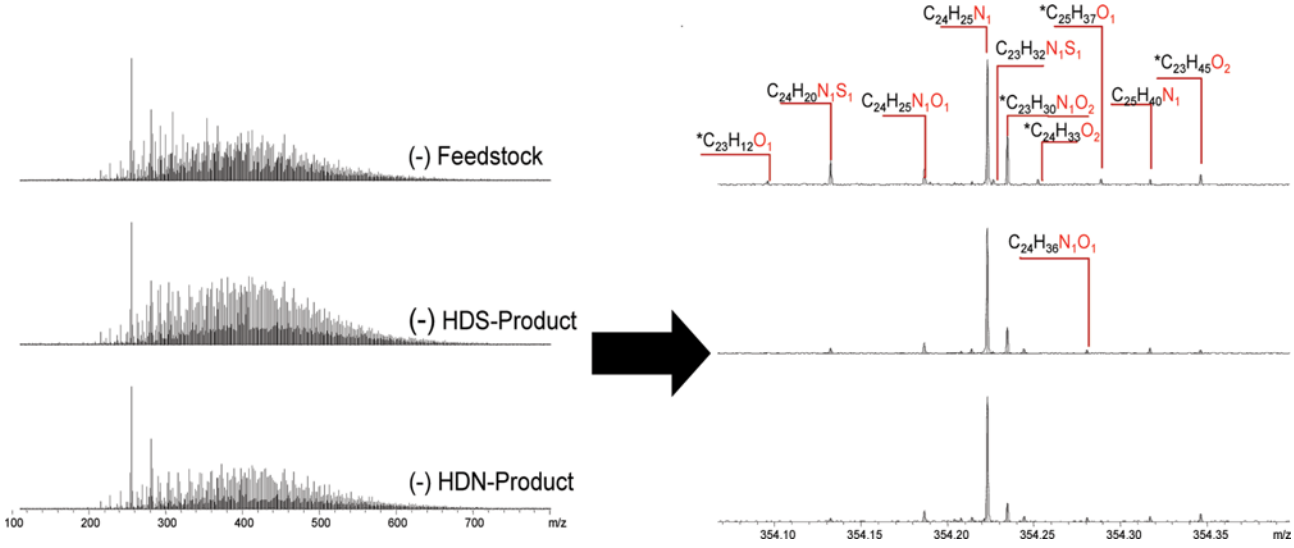

Fig. 4. Broadband negative-ion ESI FT-ICR MS mass spectra of feedstock and hydrotreating products (left), the expanded negative-ion ESI FT-ICR MS mass spectra (right).

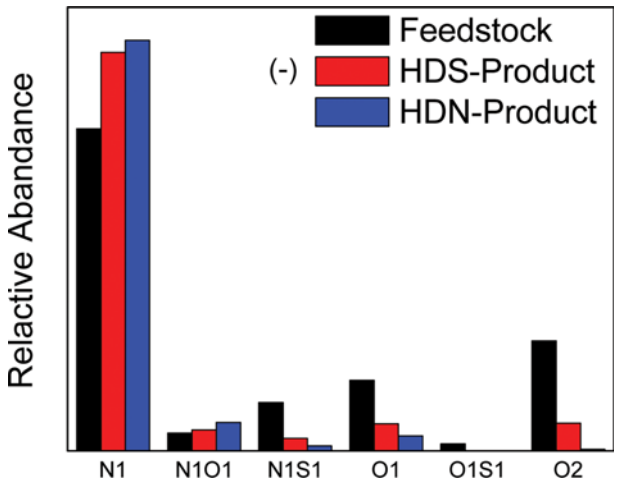

Fig. 5. Relative abundances of the dominant class species in feedstock and hydrotreating products, by negative-ion ESI FT-ICR MS.

the hydrotreating process. Moreover, the removal of small molecules was obvious; therefore, the highest peak moved backward, indicating quick conversion of neutral N_1 compounds. Eleven types of heteroatom compounds such as N_1, N_1O_1, N_1S_1, O_1, and O_2 class species were detected at m/z 354. The N_1 class species had the highest relative abundance. During the entire hydrotreatment process, the relative abundances significantly changed, because of the removal of heteroatom compounds.

Fig. 5 shows the distributions of various class species in the feedstock and hydrotreating products obtained from the negative-ion ESI FT-ICR MS from different reactor outlets. A total of six class species, N_1, N_1O_1, N_1S_1, O_1, O_1S_1, and O_2, were identified, indicating the highest relative abundance of N_1 class species in the feedstock and hydrotreated products. With increasing depth of the hydrotreating process, the relative abundances of N_1 and N_1O_1 class species increased, whereas those of N_1S_1, O_1S_1, O_1, and O_2 class species decreased, suggesting that the N_1O_1 class species are refractory to the hydrotreating process. The relative abundance increases, because of the stable π-π conjugated structure formed by the N atom in the furan ring and the aromatic ring. The increase in the relative abundance of N_1 compounds was attributed to the preferential removal of S from the N_1S_1 class species by the catalyst bed, converting to the N_1 class species. The ESI ionization source can only ionize the oxygen-containing compounds with hydroxyl groups. Meanwhile, alcohols far from the effect of ionization of phenols, the O_1 class species were basically detected as monohydric pheno-

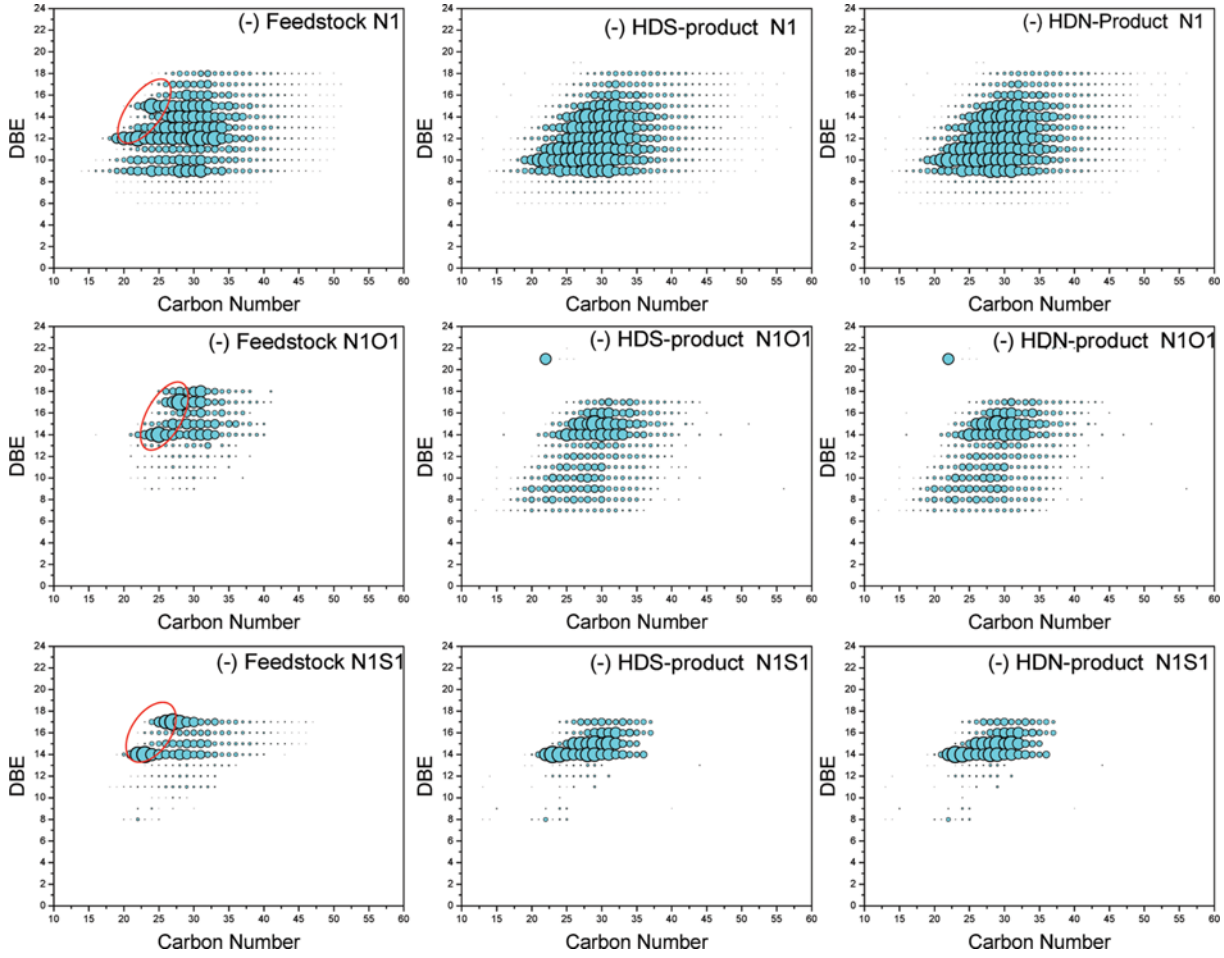

Fig. 6. DBE-carbon number for neutral N-containing compounds in feedstock and hydrotreating products.

Table 2. Representative molecular structures of neutral N_1 class species

DBE	Structural formula	DBE	Structural formula
9	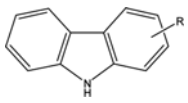	10	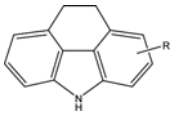
11	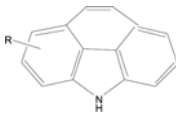	12	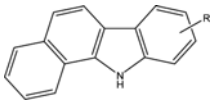
13	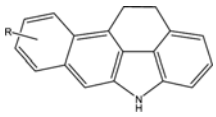	14	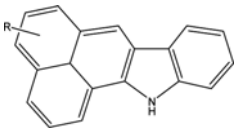
15	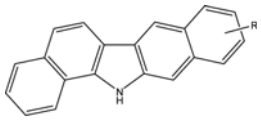	16	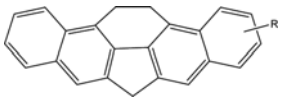
17	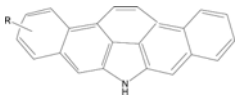	18	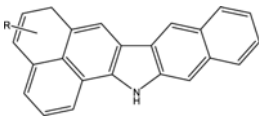

lic compounds. O_2 class species can be saturated fatty acids, naphthenic acids, phenols, or a small amount of carboxylic acid compounds, all of which can be easily removed during the hydrotreating process.

Fig. 6 shows the double bond equivalents (DBEs) - carbon number distributions of N_1, N_1O_1, and N_1S_1 class species in the feedstock and hydrotreating products. In the feedstock, N_1 class species with DBEs 9, 12, and 15 were dominant, whereas those in products were evenly distributed in the DBE range 9-18. The partial molecular structures of neutral N_1 class species are listed in Table 2. The highest aromatic ring number of neutral N_1 compounds can reach five rings. For two to five aromatic carbazoles, the substituents of the phenyl groups in the isomeric compounds were different. Due to the hydrogenation saturation effect of highly condensed compounds, some compounds with short side chains (red circle) reacted with the active sites of the catalyst because of their strong activity, thus obviously decreasing their relative abundance [27]. The relative abundance of N_1 class species was the highest at DBE=12, and the corresponding N_1S_1 and N_1O_1 class species were the highest at DBE=14. The added two DBEs were mainly ascribed to the existence of N atoms in the thiophene and furan rings. The benzene ring connected to the thiophene ring has a stable π-π conjugated structure, making the N_1S_1 and N_1O_1 class species with DBE=14 difficult to remove during the hydrotreating process. In addition, the DBE-carbon number distribution of the N_1O_1 and N_1S_1 class species shows that the higher condensation degree compounds with shorter side chains inside of the red circle had stronger hydrogenation activity and were more easily removed, and this result is consistent with the results of the N_1 class species.

3. Molecular Composition Characterized by Positive-ion ESI FT-ICR MS

The structural characteristics of the heteroatom compounds were also studied by ESI FT-ICR MS under the positive ion mode. Fig. 7 shows the broadband and the expanded mass spectra under the positive ion ESI FT-ICR MS of the feedstock and hydrotreating products from different reactor outlets. With increasing depth of the hydrotreatment reactor, the highest peak significantly shifted from m/z 380 of feedstock to m/z 420 of the products, because of stronger hydrogenation of small molecule heteroatom compounds. A total of nine heteroatom compounds including N_1, N_1O_1, and N_1S_1 class species at m/z 418 were detected. The N_1 compounds showed the highest relative abundance.

Fig. 8 shows the relative abundance of the major heteroatom compounds in the feedstock and different outlet oils obtained by further analysis of the obtained data. The N_1, N_1O_1, N_1S_2, N_2, and O_1S_1 class species were the main types of heteroatom compounds contained in the feedstock and products, with N_1 compounds with

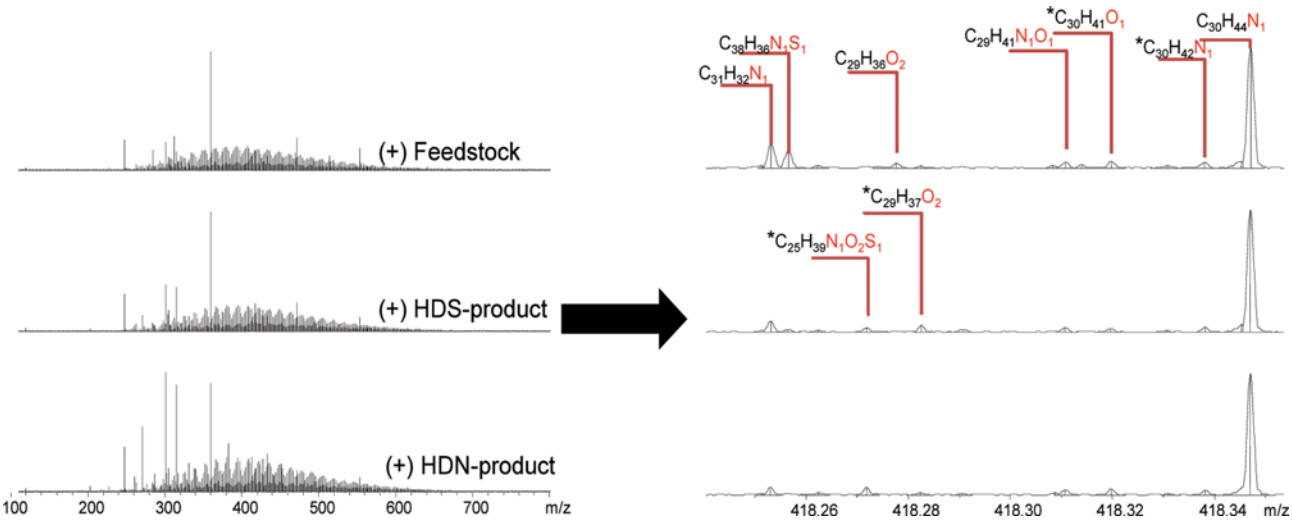

Fig. 7. Broadband positive-ion ESI FT-ICR MS of feedstock and hydrotreating products (left), the expanded positivee-ion ESI FT-ICR MS (right).

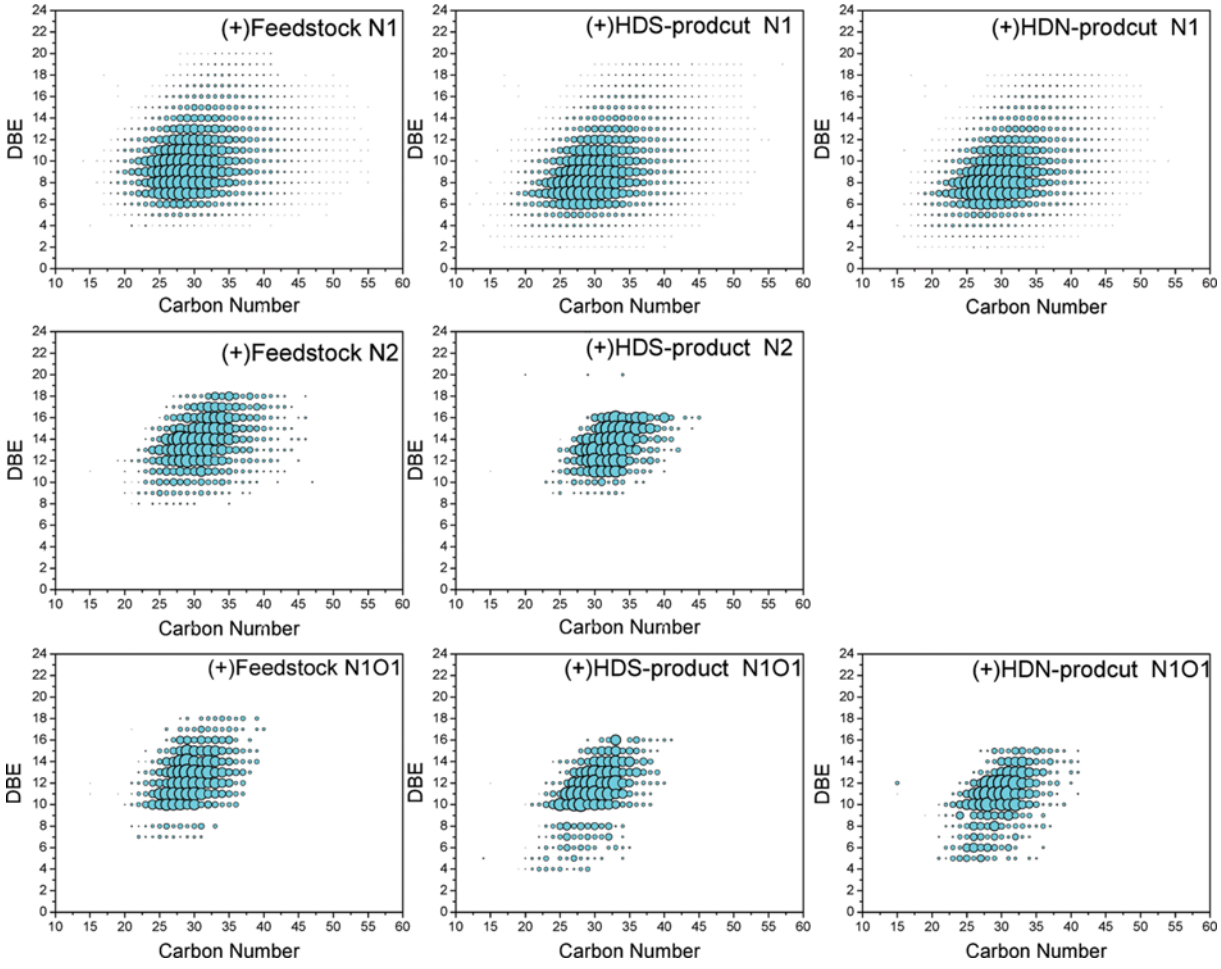

Fig. 8. Relative abundances of the dominant class species in feedstock and hydrotreating products, by positive-ion ESI FT-ICR MS.

the highest relative abundance [31]. Because amines are rarely present in crude oil [32], the basic N compounds could be pyridine derivatives [33]. Previous studies [25,34-39] suggest that hydrotreatment preferentially removes the oxygen or sulfur atoms from the N_1O_1 and N_1S_2 class species and converts them to the N_1 class species, thus increasing the relative abundance of N_1 class species in the hydrotreated products. Under the positive ion mode, sulfoxides can be directly ionized. The detected O_1S_1 and O_2S_1 compounds contain the sulfoxide structures with extremely strong hydrogenation activities and could be removed easily [25].

According to the distribution characteristics of DBE and carbon number, these basic N_1 class species have one to seven aromatic rings. These compounds contain a variety of isomers, and some of their typical structures were speculated. The details are listed in Table 3. The N_2 class species were complex in structure and could not be judged by the high-resolution data; however, they can be determined according to their DBE. The most likely molecular structures are listed in Table 4.

Fig. 9 shows the DBE-carbon number distributions of N-containing compounds, N_1, N_2, and N_1O_1 species in the feedstock and hydrotreating products, indicating that small molecule compounds enter into the catalyst pore channels more easily because of their small steric hindrance. The representative molecular structures of basic N_1 and N_2 class species are listed in Tables 3 and 4, respectively. High-DBE N-containing compounds easily hydrogenated and converted to lower-DBE compounds. By significantly reducing the low carbon number and high DBE basic N_1 class species, the mass center of gravity moved to the lower right. The N_1 class species with major relative abundance also shifted from DBE=10 to DBE=7. During the hydrotreating process, the N_2 class species first appeared at high DBE molecular hydrogenation saturation. Upon reaching at the HDN catalyst bed, the active components in the bed catalyst strongly reacted with the N-containing compounds, removing one or two N atoms, and thus no bifunctional N_2 class species were detected in the HDN products. In the feedstock, the N_1O_1 class species have DBE and the carbon number in the ranges 7-18 and 20-36, respectively. During the hydrotreating process, double bonds became saturated, shifting the center of mass downward. In contrast, because of the partial removal of one of the oxygen atoms in the N_1O_2 class species, the relative content of DBE N_1O_1 class species in the product significantly decreased.

CONCLUSION

The stepwise transformation of basic and neutral nitrogen compounds was investigated by ESI FT-ICR MS under the positive

Table 3. Representative molecular structures of basic N_1 class species

DBE	Structural formula	DBE	Structural formula
5	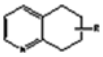	6	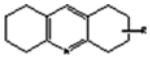
7	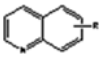	8	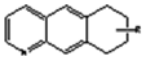
9	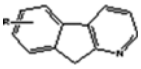	10	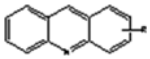
11	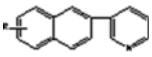	12	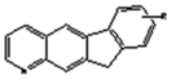
13	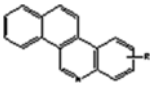	15	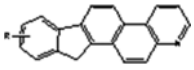
16	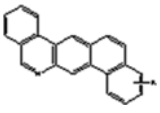	17	
18	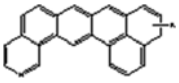	19	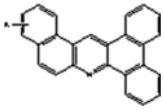
20	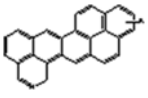	21	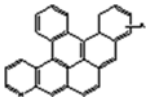

Table 4. Representative molecular structures of basic N_2 class species

DBE	Structural formula	DBE	Structural formula
8	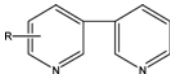	9	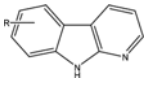
10	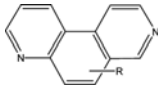	10	
12	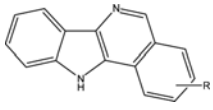	15	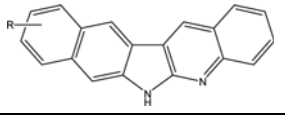

and negative ion modes. The results show that the N_1 class species account for the highest relative abundance, irrespective of the feedstock and products. The neutral N compounds were more easily removed compared to the basic N compounds. With increasing hydrogenation depth, the N_1 class species with a high condensation degree were prone to hydrogenation compared to the N_1 class species with a low condensation degree. In the feedstock, the N_1 class species with short side chains and small molecules account for a large proportion and can easily enter into catalyst pore channel and are removed by reacting with the active center. Most of the N_1S_1 class species converted to the N_1 class species because sulfur atoms were removed first. Except for those with a high condensation degree and/or short side chains, the N_1O_1 class species were difficult to remove owing to their conjugated structures, and the

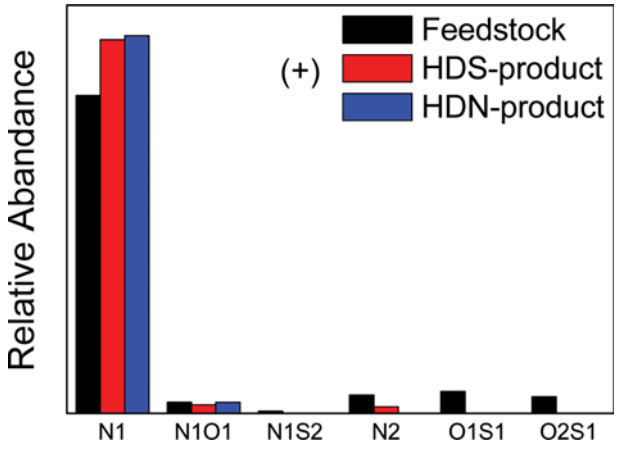

Fig. 9. Distribution of DBE and carbon number for basic N-containing compounds of feedstock and hydrotreating products.

N_2 class species have double bonds and thus are advantageous in the transformation and removal processes. Through this study, the molecular level of the residue hydrotreating transformation trends, especially the basic and neutral nitrogen-containing compounds, was found. Advanced research will be continued to provide the necessary theoretical basis for the optimum choice of residue hydrotreating conditions and catalysts.

ACKNOWLEDGEMENTS

This work was supported by the National Natural Science Foundation of China (21476101), Major Scientific Research Projects of CNOOC (HLOOFW(P)2014-0005), and scientific research cultivation fund of LSHU (520001).

REFERENCES

1. D. Liu, J. Gui, Y. K. Park, S. Yang, Y. Gao, X. Peng and Z. Sun, *Korean J. Chem. Eng.*, **29**, 49 (2012).
2. K. E. Jeong, T. W. Kim, J. W. Kim, H. J. Chae, C. U. Kim, Y. K. Park and S. Y. Jeong, *Korean J. Chem. Eng.*, **30**, 509 (2013).
3. Y. Sun, C. Yang, H. Shan and B. Shen, *Energy Fuels*, **25**, 269 (2010).
4. Y. Liu and Y. Zou, *Korean J. Chem. Eng.*, **30**, 1985 (2013).
5. A. Marafi, A. Hauser and A. Stanislaus, *Energy Fuels*, **20**, 1145 (2006).
6. L. Jiang, Y. Weng and C. Liu, *Energy Fuels*, **24**, 1475 (2010).
7. M. C. Kim and K. L. Kim, *Korean J. Chem. Eng.*, **13**, 1 (1996).
8. S. I. Andersen, J. O. Jensen and J. G. Speight, *Energy Fuels*, **19**, 2371 (2005).
9. D. Liu, T. Hou and K. Zheng, *J. Fuel Chem. Technol.*, **41**, 579 (2013).
10. K. Qian, W. K. Robbins, C. A. Hughey, H. J. Cooper, R. P. Rodgers and A. G. Marshall, *Energy Fuels*, **15**, 1505 (2001).
11. W. Liang and G. Que, *Acta Petrolei Sinca (Petroleum Processing Section)*, **1**, 1 (1991).
12. M. Canel, E. Canel, A. G. Borrego, C. G. Blanco and M. D. Guillén, *Fuel Process Technol.*, **43**, 111 (1995).
13. S. I. Andersen and K. S. Birdi, *Fuel Sci. Technol. International*, **8**, 593 (1990).

14. J. M. Purcell, C. L. Hendrickson, R. P. Rodgers and A. G. Marshall, *Anal. Chem*., **78**, 5906 (2006).
15. R. P. Rodgers and A. M. Mckenna, *Anal. Chem*., **83**, 4665 (2011).
16. F. A. Fernandez-Lima, B. Christopher, A. M. Mckenna, R. P. Rodgers, A. G. Marshall and D. H. Russell, *Anal. Chem*., **81**, 9941 (2009).
17. B. Amit, T. Haim and M. Daniel, *Anal. Chem*., **81**, 8627 (2009).
18. K. Qian, R. P. Rodgers, C. L. Hendrickson, M. R. Emmett and A. G. Marshall, *Energy Fuels*, **15**, 492 (2001).
19. M. J. Teräväinen, J. M. H. Pakarinen, K. Wickström and P. Vainiotalo, *Energy Fuels*, **21**, 266 (2006).
20. D. F. Smith, G. C. Klein, A. T. Yen, M. P. Squicciarini, R. P. Rodgers and A. G. Marshall, *Energy Fuels*, **22**, 3112 (2008).
21. Q. Shi, D. Hou, K. H. Chung, S. Zhao and Y. Zhang, *Energy Fuels*, **24**, 2545 (2010).
22. L. Zhang, Z. Xu, S. Quan, X. Sun, N. Zhang, Y. Zhang, K. H. Chung, C. Xu and S. Zhao, *Energy Fuels*, **26**, 5795 (2012).
23. Y. Zhang, L. Zhang, Z. Xu, N. Zhang, K. H. Chung, S. Zhao, C. Xu and Q. Shi, *Energy Fuels*, **28**, 7448 (2014).
24. H. Müller, J. T. Andersson and W. Schrader, *Anal. Chem*., **77**, 2536 (2005).
25. J. Fu, G. C. Klein, D. F. Smith, S. Kim, R. P. Rodgers, C. L. Hendrickson and A. G. Marshall, *Energy Fuels*, **20**, 1235 (2006).
26. L. Dong, F. Yue, W. Deng, Q. Shi, K. Ma, T. Hou and C. Wu, *Energy Fuels*, **26**, 624 (2011).
27. T. Zhang, L. Zhang, Y. Zhou, Q. Wei, K. H. Chung, S. Zhao, C. Xu and Q. Shi, *Energy Fuels*, **27**, 2952 (2013).
28. J. M. Purcell, I. Merdrignac, R. P. Rodgers, A. G. Marshall, T. Gauthier and I. Guibard, *Energy Fuels*, **24**, 2257 (2009).
29. M. Liu, M. Wang, L. Zhang, Z. Xu, Y. Chen, X. Guo and S. Zhao, *Energy Fuels*, **29**, 702 (2015).
30. Q. Shi, C. Xu, S. Zhao, K. H. Chung, Y. Zhang and W. Gao, *Energy Fuels*, **24**, 563 (2009).
31. Q. Hu, Y. Liu, Z. Liu, S. Tian and Z. Xu, *Chinese J. Anal. Chem*., **38**, 564 (2010).
32. A. M. McKenna, J. M. Purcell, R. P. Rodgers and A. G. Marshall, *Energy Fuels*, **24**, 2929 (2010).
33. J. H. Chang, E. S. Ko, S. H. Park and K. L. Kim, *Korean J. Chem. Eng*., **12**(2), 176 (1995).
34. K. Qian and S. H. Chang, *Anal. Chem*., **64**, 2327 (1992).
35. H. Yu, S. Li and G. Jin, *Energy Fuels*, **24**, 4419 (2010).
36. D. Zhao, W. Sun and M. Sun, *Petrol. Sci. Technol*., **29**, 2530 (2011).
37. X. Chen, B. Shen, J. Sun, C. Wang, H. Shan, C. Yang and C. Li, *Energy Fuels*, **26**, 1707 (2012).
38. R. J. Angelici, *Polyhedron*, **16**, 3073 (1997).
39. G. C. Klein, R. P. Rodgers and A. G. Marshall, *Fuels*, **85**, 2071 (2006).